



Trans. Nonferrous Met. Soc. China 32(2022) 461-471

Transactions of Nonferrous Metals Society of China

www.tnmsc.cn



Laser-induced combustion joining of C_f/Al composites and TC4 alloy

Guang-jie FENG^{1,2}, Zhuo-ran LI¹, Peng HE¹, Lei SHEN¹, Zhi ZHOU¹

State Key Laboratory of Advanced Welding and Joining, Harbin Institute of Technology, Harbin 150001, China;
College of Materials Science and Engineering, Chongqing University, Chongqing 400044, China

Received 21 February 2021; accepted 14 September 2021

Abstract: The C_f/Al composites were joined to the TC4 alloy via the laser-induced combustion joining method. The exothermic reaction of the interlayer provided the required energy for the joining process. By combining the theoretical calculation and experiment, the chemical composition of the Ni–Al–Zr interlayer was designed. The microstructure and mechanical properties of the joint were investigated. The results show that the addition of Zr slightly weakened the combustion reaction of exothermic interlayer but played a key role in the successful joining. Ni–Al–Zr interlayer reacted with substrates, forming a TiAl₃ layer adjacent to TC4 alloy and NiAl₃, Ni₂Al₃ layers adjacent to the C_f/Al composites. Zr content dominated the microstructure and shear strength of the joint. When the Zr content was 5 wt.% under the joining pressure of 2 MPa, the joint had a maximum shear strength of 19.8 MPa.

Key words: C_f/Al composites; TC4 alloy; combustion joining; interfacial microstructure; shear strength

1 Introduction

Carbon fiber reinforced aluminum matrix composites (C_f/Al composites) have attracted great attention because of their outstanding properties (i.e. good dimensional stability, lightweight, high stiffness and strength, and excellent thermal conductivity) [1-4]. However, the high processing difficulty of the C_f/Al composites limits their practical applications [5]. Joining the C_f/Al composites to other materials, especially to metals and alloys, can overcome the disadvantages [6,7]. TC4 alloy has been widely applied in aerospace fields because of its low density, good workability, excellent corrosion resistance, and outstanding fracture toughness [8-10]. The reliable joining of C_f/Al composites and TC4 alloy can produce structures with combined advantages, thus further extending their applications.

Joining the C_f/Al composites to TC4 alloy is a great challenge. Firstly, the C_f/Al composites are

very sensitive to temperature and pressure. Research on C_f/Al composites reveals that high pressure and long-time heat treatment above 823 K can cause the microcrack initiation at the carbon fiber/aluminum matrix interface and excess interfacial chemical reaction, respectively [11-14]. Secondly, there is a great CTE (coefficient of thermal expansion) mismatch between these two materials. The CTE of the TC4 alloy is $8.8 \times 10^{-6} \,\mathrm{K}^{-1}$ [15], which is quite different from that of the C_f/Al composites (transverse CTE of (17-20)×10⁻⁶ K⁻¹, and longitudinal CTE of $0.27 \times 10^{-6} \,\mathrm{K}^{-1}$) [16]. The above two aspects demonstrate that the conventional welding methods cannot give satisfactory results. Fusion welding, diffusion welding, and friction welding will lead to the mass generation of brittle Al₄C₃ compounds and microcracks in the C_f/Al substrate, resulting in the degradation of materials properties. Brazing, which is a frequently-used method to join dissimilar materials [17], is also inapplicable to the joining of C_f/Al composites and TC4 alloy due to the lack of appropriate filler metals. To solve this problem, developing a new joining method is of great necessity.

Combustion joining utilizes the combustion synthesis (CS) reaction of the exothermic interlayer to join materials [18]. During the combustion joining, the exothermic reaction occurs in the interlayer, and only heats the surface of the substrates to a high temperature rapidly (10⁵– 10⁶ K/s), while other region remains at a relatively low temperature. It merely affects the region near the interlayer, thus avoiding the thermal damage of the base metal. Meanwhile, the interlayer products with desired properties can also be in-situ synthesized and serve as a gradient layer to relieve the CTE mismatch of dissimilar materials [7,19]. In previous research, the Ni-Al interlayer was widely used as an exothermic system. PASCAL et al [20] have successfully synthesized NiAl alloys and realized the simultaneous joining with a superalloy substrate by CS using an equimolar mixture of nickel and aluminum powders. LONG et al [21] realized the transient liquid phase bonding of copper and alumina ceramics with the Ni/Al nano multilayers. Our preliminary study [7] indicated that when joining C_f/Al composites with Ni-Al interlayer, the interfacial reaction between the interlayer and carbon fibers was very weak, leading to poor joining quality. Research on joining C/C composites showed that carbide forming elements (Ti, Zr, etc) could enhance the interfacial reaction between carbon fibers and filler metals [22]. Thus, when joining the C_f/Al composites to TC4 alloys with the assistance of exothermic reaction, appropriate Ti or Zr should be added into the Ni-Al system.

In this work, a Ni–Al–Zr interlayer was designed based on theoretical calculation and DSC analysis. To mitigate the possible thermal damage on the C_f/Al composites during the ignition process, a laser beam was applied in consideration of its small heating area and high heating rate. The joining of C_f/Al composites and TC4 alloys was realized via the laser-induced combustion joining method. The interfacial reactions and the joint shear strength were investigated systematically. Moreover, the optimal joining parameters were achieved by revealing the correlation between the joint microstructure and joint shear strength.

2 Experimental

The C_f/Al composites were provided by the Harbin Institute of Technology Composites Materials Research Institute. The metal matrix was 6061 aluminum alloy, and the carbon fiber had a volume fraction of 50%. Figure 1 shows the microstructures of the C_f/Al composites. TC4 alloy had a nominal composition of Ti–6Al–4V (wt.%). Prior to the joining, the C_f/Al composites and TC4 alloy were cut into small pieces with the sizes of 5 mm × 5 mm × 3 mm and 8 mm × 15 mm × 1.5 mm, respectively. Then, all the bonding surfaces were polished using sandpaper up to 1000# grit and cleared in acetone for 10 min with the assistance of ultrasonic to remove the impurities.

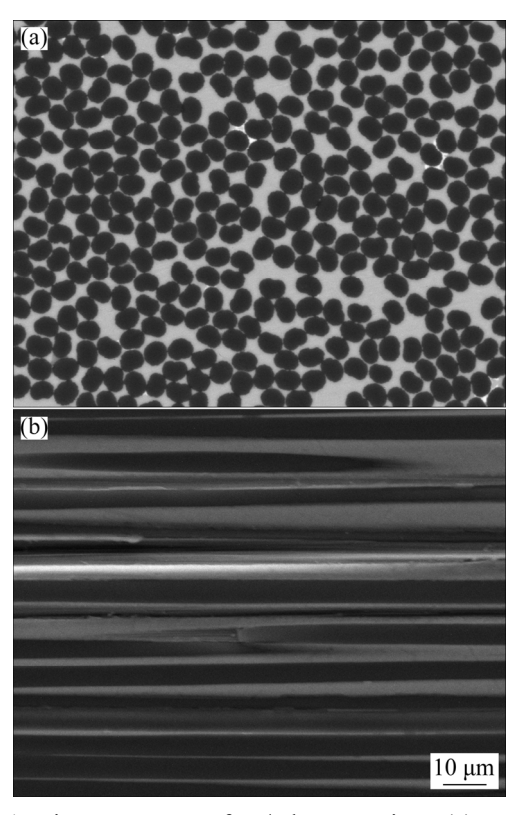


Fig. 1 Microstructures of C_f/Al composites: (a) Vertical to carbon fiber; (b) Parallel to carbon fiber

High purity powders of Ni (99.5%, $28 \mu m$), Al (99.5%, $28 \mu m$), and Zr (99.5%, $28 \mu m$) were used to prepare the powder interlayer. The weighed powders were put into an agate jar and milled with alumina balls for 60 min in an argon atmosphere. The rotational speed was set to be 300 r/min and the mass ratio of ball to powders was 10:1. Then, 0.5 g milled powders were cold-pressured to a cylindrical

compact (d=10 mm, h=1.3 mm). The joining process was conducted in an argon atmosphere. Figure 2 represents the joining schematic diagram. During the joining, a powder interlayer was applied between the C_f/Al and TC4 substrates. A special fixture was used to provide the joining pressure. A laser beam (IPG Photonics Corporation, YLR-100-AC, P=100 W) heated the interlayer for 5 s. The exothermic reaction was ignited and the joining process was finished.

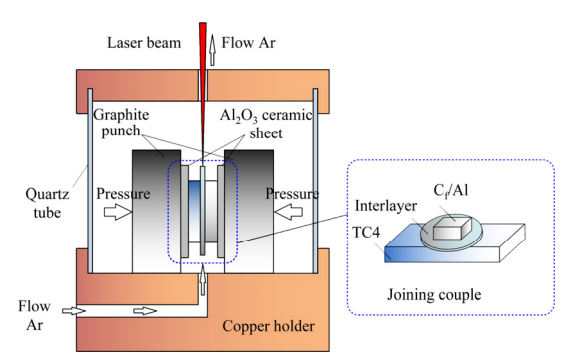


Fig. 2 Joining schematic diagram

The exothermic performance of interlayer, the joint interfacial microstructure, and interlayer products were characterized by the differential scanning calorimeter (DSC, TGA/DSC/1600LF), scanning electron microscope (SEM, Hitachi S-4700) equipped with the energy-dispersive spectrometer (EDS), X-ray diffractometer (XRD, D8 ADVANCE), and transmission microscope (TEM, Talos F200x). Before the XRD test, the C_f/Al composites were removed by grinding until the interlayer products were reached. Then, the sample was subjected to the XRD procedure. The room temperature shear strength of the joint was tested using the universal test machine (Instron-1186). The shear rate was set to be 0.5 mm/min. Figure 3 shows the schematic diagram of the joint shear test.

3 Results and discussion

3.1 Design of Ni-Al-Zr interlayer

In this study, to mitigate the possible thermal damage on the C_f/Al composites during the ignition, a laser beam was employed to ignite the self-propagating exothermic reaction of the interlayer. It requires that the exothermic system should have a low reaction activation energy and release enough heat to self-sustain the exothermic reaction [23].

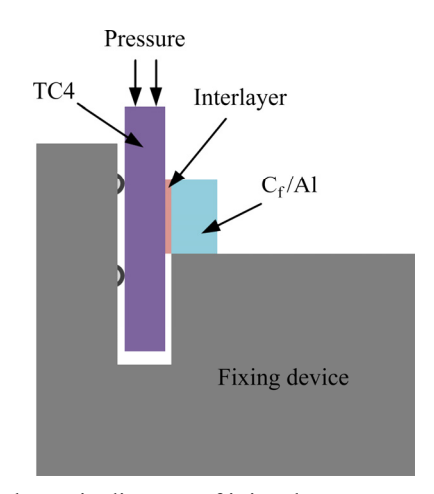


Fig. 3 Schematic diagram of joint shear test

Investigations on the combustion synthesis show that the Ni-Al system could meet the requirement [24]. Firstly, Ni-Al exothermic reaction begins with the reaction (Ni+3Al=NiAl₃, ΔH =-150.624 kJ/mol), which has a low reaction activation energy of (119.22±10.72) kJ/mol [25]. Secondly, the exothermicity and reaction products of the Ni-Al system are able to be tailored by changing the Ni/Al molar ratio. In the combustion synthesis field, the adiabatic temperature (T_{ad}) offers a useful metric to evaluate the exothermicity of an exothermic system [26]. For the laser-induced self-propagating mode in this study, $T_{ad} \ge 1800 \text{ K}$ is considered as the empirical critical condition [27]. To predict the possible effect of the exothermic reaction, the $T_{\rm ad}$ of the Ni–Al system with different Ni/Al molar ratios was obtained according to the following equation:

$$\Delta H(298) + \int_{298}^{T_{ad}} \sum_{j} n_j c_p(P_j) dT + \sum_{j=0}^{T_{ad}} n_j L(P_j) = 0$$

where T, P_j , n_j , $c_p(P_j)$, and $L(P_j)$ are the thermodynamic temperature, products, stoichiometric coefficients, the specific heat capacity, and phase transformation enthalpy (if a phase change occurs), respectively.

The calculation results show that when the Ni/Al molar ratio is 1:1, the $T_{\rm ad}$ reaches the maximum of 1912 K. According to the empirical criterion, a self-propagating combustion wave could be formed. To verify the above theoretical analysis, an interlayer was fabricated with equimolar Ni and Al powders. After being ignited, a stable combustion wave was observed. Thus, the equimolar Ni–Al system was selected as the basic

exothermic system.

In combustion joining, the joining quality depends on the interfacial reactions between the interlayer and substrates. The corresponding phase diagrams and research indicate that the Ni-Al system has a high affinity with aluminum and TC4 alloy, and stable reaction layers can be formed at the Ni-Al/aluminum and Ni-Al/TC4 interfaces. While for the Ni-Al/carbon fiber reaction couple, no stable reaction layers can be formed due to their weak chemical affinity with each other. Investigations on brazing C/C composites showed that carbide forming elements (Ti, Zr, etc) enhanced the interfacial reactions between carbon fiber and filler metals [28]. Referring to the previous research [5,17], Zr was added in the equimolar Ni-Al system, forming the Ni-Al-Zr system. The addition of Zr will influence the interlayer in two aspects. On the one hand, Zr will promote the reactions between the interlayer and carbon fibers [5,29], improving the joining quality. On the other hand, Zr will work as a diluent to absorb the reaction heat and reduce the released heat from the exothermic reaction. To predict the effect of Zr addition on the exothermicity, the $T_{\rm ad}$ of the Ni-Al-Zr system with different Zr additions was calculated. When the Zr addition was lower than 44.48 wt.%, the $T_{\rm ad}$ was higher than 1800 K and reached the empirical critical condition (1800 K) for a self-sustaining exothermic reaction. Therefore, the Zr addition was determined to be 0-44.48 wt.%.

Figure 4 gives the DSC curves of the Ni-Al and Ni-Al-Zr interlayers. In the curve of the Ni-Al interlayer, an exothermic peak at 912 K was observed. It indicated that the ignition temperature was about 912 K. After adding some Zr, the exothermic peak location shifted from 912 to 903 K, which meant that the ignition temperature was decreased by 9 K and the interlayer could be ignited more easily by a laser beam. The formation of this phenomenon is hypothesized as follows. Due to the high chemical affinity between Al and O, there is an alumina layer formed around the Al particle. It impedes the interdiffusion between the Ni and Al. A high temperature is required to provide enough driving force for the atomic interdiffusion and ignite the exothermic reaction. Since Zr is an active element, it can react with the alumina layer, thus reducing the disadvantageous influence of the alumina layer on the atomic interdiffusion. As a consequence, the activation energy of the ignition process and the ignition temperature decreased. Meanwhile, the Zr addition lowered the height of the exothermic peak. In the Ni–Al–Zr system, the main exothermic reactions were the reactions between Ni and Al, while the reactions between Zr and Ni (or Al) only released a small amount of heat. So, the total heat released from the exothermic system decreased, leading to the decrease of the peak height. Although the Zr addition lowered the exothermicity of the interlayer, the adiabatic temperature was still higher than 1800 K. Therefore, the self-sustain exothermic reactions and the interfacial reactions could be guaranteed.

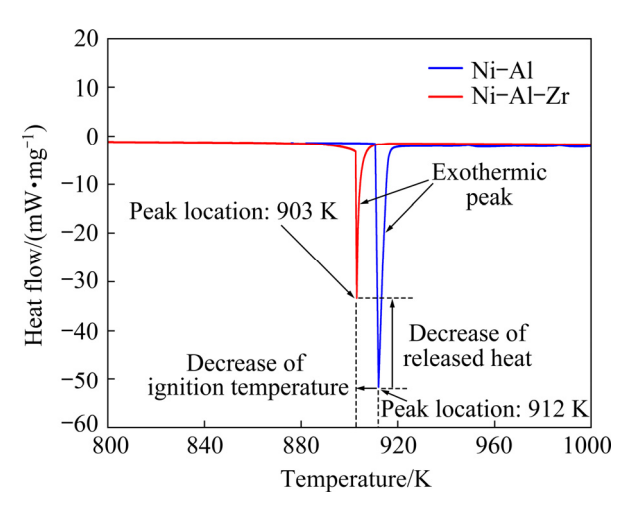


Fig. 4 DSC curves of Ni–Al and Ni–Al–Zr interlayers (5 wt.% Zr, 10 K/s, and Ar atmosphere)

3.2 Joint microstructure

3.2.1 TC4/Ni-Al/(C_f/Al) joint

Figure 5 shows the microstructure of the joint bonded with the Ni-Al interlayer under 2 MPa. The gray interlayer products were produced and a metallurgical bonding was formed with the adjacent substrates. In the interlayer products, one can find the defects such as pores, residual reactant phases (clastic texture dispersed in the dark grey matrix). On the C_f/Al composites side, some microcracks were observed near and at the interlayer/composites interface (see Fig. 5(b)). Three reasons may contribute to defects in the reaction products, which were: (1) pores present in the original compact, (2) unevenly mixing of Al powder and Ni powder leading to residual reactant phases, and (3) unbalanced diffusivity between Al and Ni, respectively. According to the analysis in Section 3.1, the theoretical products of the Ni–Al interlayer

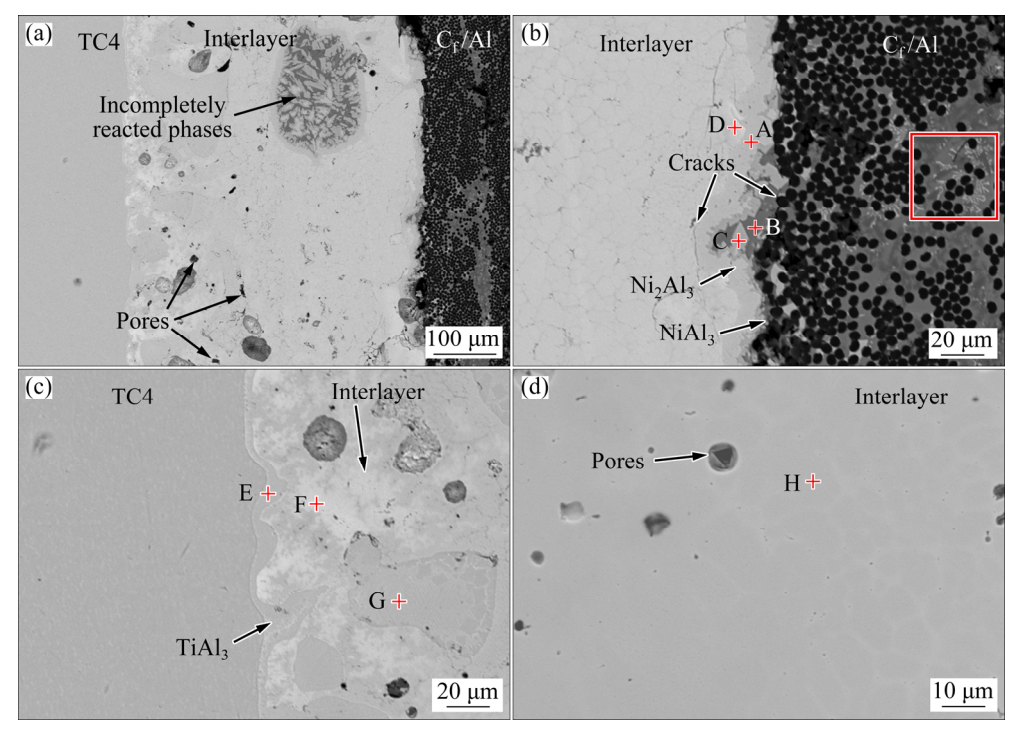


Fig. 5 Microstructures of TC4/Ni-Al/(C_f/Al) joint: (a) Overall view; (b) C_f/Al side; (c) TC4 side; (d) Joint center

were NiAl intermetallics. Its melting point was 1912 K, which was as high as the $T_{\rm ad}$ of the Ni–Al interlayer. Theoretical calculation indicated that the NiAl products were in the solid–liquid coexistence state with a melting rate of 42%. The fraction of liquid phases was certainly lower than 42% in the actual situation. During the joining, the voids in the interlayer cannot be fully filled due to the shortage of the liquid phases, forming the pores in the products.

Figures 5(b-d) show the details in the joint, while Table 1 gives the EDS results of different phases. Thermodynamic calculations suggested that the $T_{\rm ad}$ of Ni–Al interlayer was as high as 1912 K. During the joining, the aluminum matrix adjacent to the interlayer melted. The interlayer reacted with melted Al matrix and two reaction layers were formed (marked by A and C, see Fig. 5(b)), which were identified as Ni₂Al₃ and NiAl₃ according to their stoichiometric ratios and previous study. The melting of the aluminum matrix promoted the diffusion of the Ni atoms, forming the small block NiAl₃ dispersed in the composites (see the red rectangle in Fig. 5(b)). Near TC4 alloy, an irregularly shaped reaction layer (Spot E, 5–8 μm in thickness) was formed due to intensive interactions between TC4 alloy and Ni-Al interlayer. EDS results show that this reaction layer was supposed

Table 1 EDS results of spots in Fig. 5

Spot		Conte	D '11 1		
	Ni	Al	Ti	V	Possible phase
A	44.11	55.89	-	_	Ni ₂ Al ₃
В	0.58	97.84	1.33	0.25	Al matrix
C	19.28	79.51	0.33	0.20	$NiAl_3$
D	60.22	39.78	_	_	Ni-rich NiAl
E	2.36	24.86	70.37	2.41	Ti_3Al
F	53.32	40.15	5.22	1.31	Ni-rich NiAl
G	41.51	55.89	2.60	_	NiAl
Н	41.87	56.21	1.92	_	NiAl

to be Ti₃Al. Observing Figs. 5(b-d), one could also find that the interlayer products were not homogeneous in the joint. In the center of the joint, the interlayer products were grey (see Fig. 5(d)). While near the substrates, there were some white phases adjacent to the reaction layers. EDS analysis on the four zones (marked by D, F, G, and H) revealed that these phases were mainly composed of Ni and Al, and their Ni content ranged from 40 at.% to 61 at.%. According to the XRD results of the interlayer products (see Fig. 6), these phases were identified as NiAl. The difference of Ni content was mainly because of the insufficient atom diffusion in these zones under the rapid heating

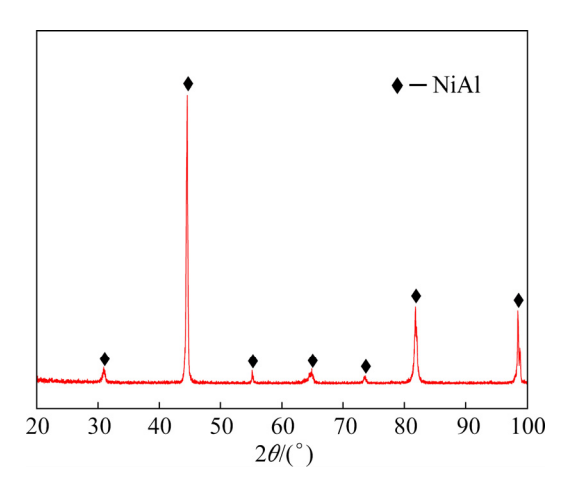


Fig. 6 XRD pattern of interlayer products

and cooling conditions. More Ni atoms were kept in the zones near the substrates, forming the white Ni-rich NiAl.

3.2.2 (C_f/Al)/Ni-Al-Zr/TC4 joint

Figure 7(a) shows the microstructures of the joint bonded with the Ni–Al–Zr interlayer under 2 MPa. After adding some Zr in the interlayer, the joint morphology underwent a dramatic change. The cracks disappeared in the joint. The size and quantity of the pores decreased significantly. Figures 7(b–f) illustrate the elemental distribution in the joint. It could be seen that Ni was mainly distributed in the interlayer products. But the distribution of Ni was different on both sides near

the substrates. On the TC4 side, the substrate/interlayer interface was quite clear. While on the C_f/Al side, the bond was much indistinct. This is because the TC4 alloy has a much higher melting point (~1933 K) than the aluminum matrix (900 K). Under the influence of exothermic reaction, the Al matrix melted locally and greatly enhanced the diffusion of Ni atoms to the aluminum matrix. Compared with the C_f/Al composites, the melting quantity of TC4 alloy was much smaller. Only a thin Ti-rich layer was formed adjacent to the TC4 alloy (see the green layer in Fig. 7(d)).

Figure 8 shows the joint microstructures in detail. Table 2 gives the EDS results of different phases. From Fig. 8(c), it could be seen that TC4 alloy joined well with the interlayer, forming a reaction layer (Spot E, 3–5 µm in thickness). The EDS results indicated that this reaction layer was Ti_3Al (the same as the interlayer in Fig. 6(c)). Near the Ti₃Al layer, there were also some light gray phase (Spot F), grey phase (Spot G) and blockshaped phase (Spot H). They were confirmed to be the Ni-rich NiAl, Ni-Al-Ti compounds and NiAl, respectively. On the C_f/Al side, the melted aluminum matrix reacted with Ni and Zr atoms from interlayer, forming the Ni₂Al₃ (Spot B) and NiAl₃ (Spot C) layers. Moreover, some needle-like phases (Spot D) were observed at the interface, which should be (Ni,Zr)Al₃ phases. Meanwhile,

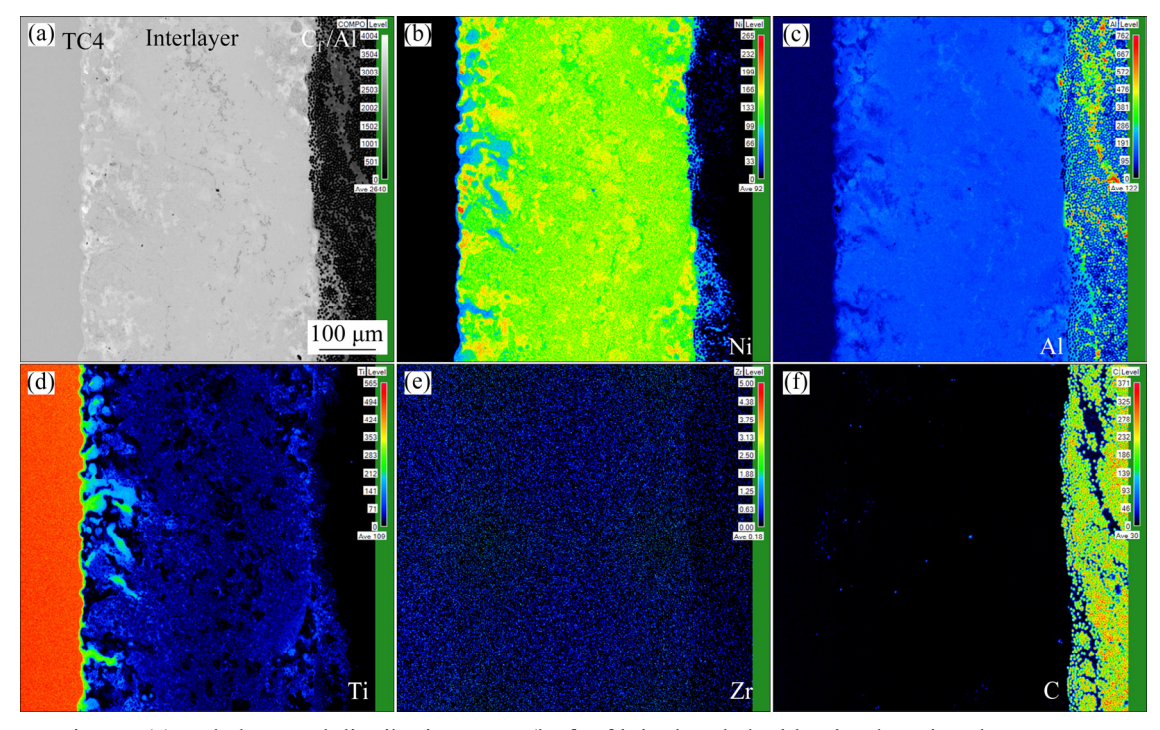


Fig. 7 SEM image (a) and elemental distribution maps (b-f) of joint bonded with Ni-Al-Zr interlayer

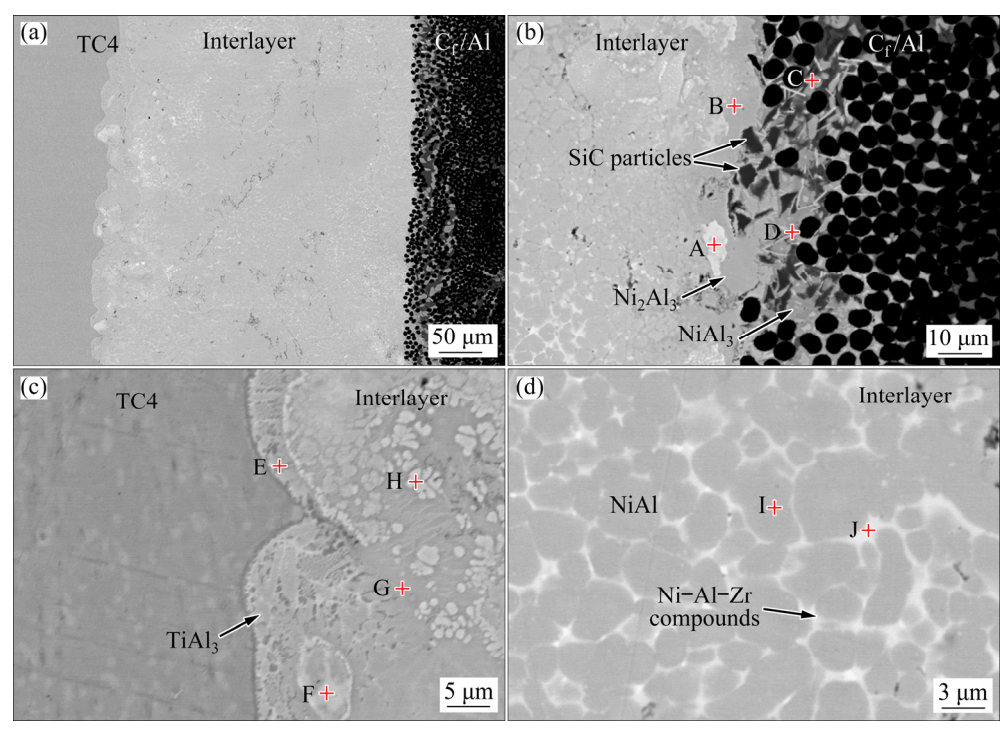


Fig. 8 Microstructures of joint bonded with Ni-Al-Zr interlayer: (a) Overall view; (b) C_f/Al side; (c) TC4 side; (d) Joint center

Table 2 EDS results of spots in Fig. 8

Spot		Co	Possible			
	Ni	Ti	Al	Zr	V	phase
A	56.33	_	40.26	3.41	_	Ni-rich NiAl
В	38.4	_	60.58	1.02	_	Ni_2Al_3
C	24.12	_	75.22	0.66	_	$NiAl_3$
D	14.43	-	74.16	11.41	_	(Ni,Zr)Al ₃
E	_	72.13	24.29	0.33	3.25	Ti ₃ Al
F	55.46	_	43.26	1.28	_	Ni-rich NiAl
G	30.77	30.06	39.17	_	_	Ni-Al-Ti compounds
Н	46.54	3.90	49.57	_	-	NiAl
I	48.52	_	49.32	2.16	_	NiAl
J	41.23	-	38.56	20.18	-	Ni-Al-Zr compounds

some SiC particles were also observed in Fig. 8(b). It should be noticed that these SiC particles were from the sand paper during the sample preparation and they were not interfacial products.

Figure 8(d) shows the morphology of the interlayer products. After adding a small amount of Zr, the interlayer products consisted of the gray block phase (Spot I) and white reticular phase (Spot J), and presented a eutectic morphology. EDS results show that the gray block phase should be

NiAl phase since the molar fractions of Ni and Al were near equal. The white reticular phase should be Ni-Al-Zr compounds. In order to further characterize the interlayer products, the interlayer products were examined by the TEM and XRD analysis. Figure 9(a) shows the TEM micrograph of the Ni-Al-Zr interlayer products. It was revealed that the interlayer products were composed of three phases, which were NiAl (black phase), Ni₃Al₅Zr₂ (gray phase) and Ni₂AlZr (white phase), repectively. This meant that the Ni-Al-Zr compounds (Spot J in Fig. 8(d)) were a mixture of Ni₃Al₅Zr₂ and Ni₂AlZr phases. Figure 9(b) shows the XRD data of the interlayer products, which also proved above analysis. Thus, the typical joint microstructure was TC4/Ti₃Al + Ni-Al-Ti + Ni-rich NiAl/Ni₂AlZr + $Ni_3Al_5Zr_2 + NiAl/Ni-rich NiAl/Ni_2Al_3/NiAl_3 +$ $(Ni,Zr)Al_3/C_f/Al.$

3.3 Effect of Zr content on joint microstructure and shear strength

Figure 10 illustrates the effect of Zr content on the joint microstructure. The Zr content influenced the joining in three aspects. Firstly, the addition of Zr transformed the interlayer products from NiAl to NiAl + Ni₃Al₅Zr₂ + Ni₂AlZr eutectic structure. During the joining, the eutectic structure could be

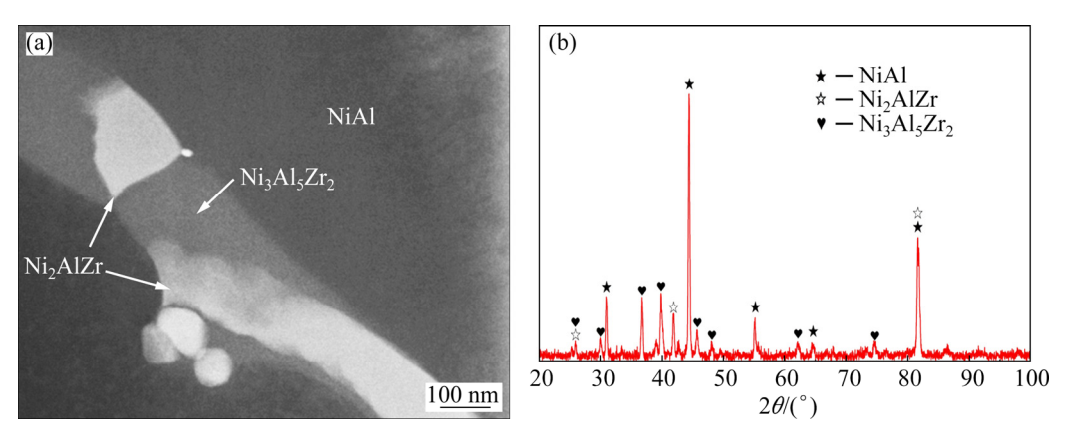


Fig. 9 TEM image (a) and XRD pattern (b) of Ni-Al-Zr interlayer products

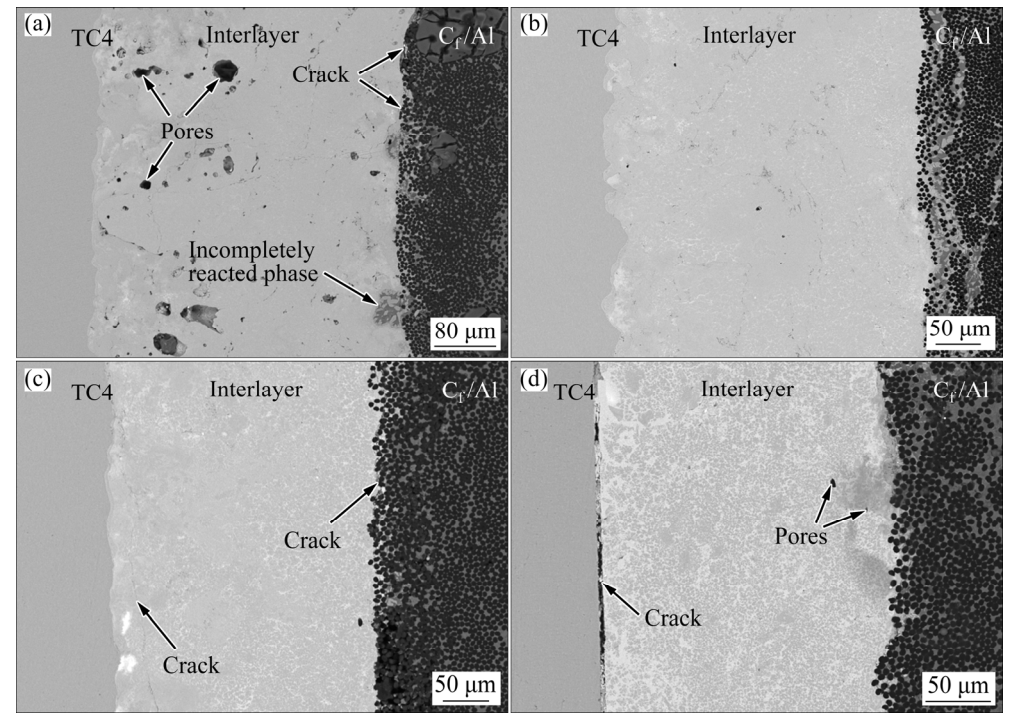


Fig. 10 Microstructures of joints with different Zr contents: (a) 1.5 wt.%; (b) 5 wt.%; (c) 10 wt.%; (d) 20 wt.%

densified more easily under the joining pressure, effectively reducing the pores in the joint. High Zr content elevated the percentage of eutectic structure and promoted the densification process. It could be seen from Figs. 10(a) and (b) that with increasing Zr content, the number of pores and their size decreased obviously. Secondly, the Zr content influenced the interlayer exothermicity and the interfacial reactions. The higher the Zr content was, the lower exothermicity the interlayer had. The change of TC4/interlayer interface morphology well displayed this effect. When the Zr content was low (1.5 wt.% and 5 wt.%), the exothermicity of the interlayer was relatively high. During the joining, the TC4 melted locally, forming a thick reaction

layer and a curved interface. Further increasing Zr content lowered the interlayer exothermicity dramatically. The melting area of the TC4 substrate became smaller, forming a straight interface. Thus, the interfacial reaction between the TC4 substrate and the interlayer became weak. The thickness of the TiAl₃ reaction layer had an obvious drop, weakening the bonding and forming the crack (see Fig. 10(d)) when the Zr content was 20 wt.%. Thirdly, the Zr content determined the interfacial reaction between the interlayer products and the carbon fibers. Thermodynamic calculations showed that the Ni–Al products had a low chemical affinity with carbon fibers and no reliable reaction layer could be formed at the interlayer/carbon fiber

interface. Thus, the bonding between the C_f/Al composites and the Ni-Al interlayer was very weak. Since Zr is a carbide forming element, its reaction with C is spontaneous thermodynamically ($Zr+C \rightarrow$ ZrC, ΔG^{Θ} =-193.27 kJ/mol). With the addition of Zr, a thin Zr-C reaction layer was produced at the interface, thus improving the bonding between the carbon fiber and the interlayer products. High Zr content further enhanced the interfacial reaction and the bonding strength. Thus, with increasing the Zr content, the crack and unconnected disappeared gradually. However, when the Zr content was excessive, the Ni-Al-Zr compounds extended into the C_f/Al composites. Continuous cracks were formed again because of the CTE mismatch and the brittle interlayer products.

Figure 11 shows the influence of Zr content on the joint shear strength. It could be seen that with increasing the Zr content, the joint shear strength increased firstly and then decreased. The joint shear strength was determined by the joint microstructure. Before adding Zr in the interlayer, the interlayer had the highest exothermicity and could provide sufficient heat for the joining process. However, the interlayer products had a low affinity with the carbon fiber and could not be fully densified during the joining. The formation of cracks and pores seriously affected the joint strength. The addition of Zr promoted the interfacial reaction between the carbon fiber and the interlayer. Meanwhile, the interlayer products transformed from NiAl to NiAl + Ni₃Al₅Zr₂ + Ni₂AlZr eutectic. Under the joining pressure, the eutectic structure was densified more easily. Thus, with increasing the Zr content, the cracks and pores disappeared gradually. The shear strength had an obvious increase and

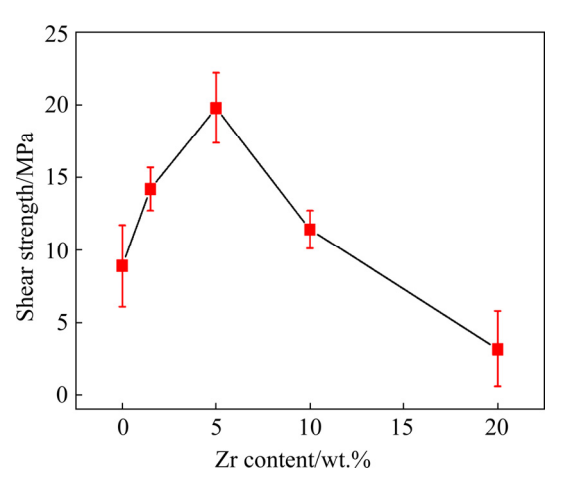


Fig. 11 Effect of Zr content on joint shear strength

reached the highest value of 19.8 MPa when the Zr content was 5 wt.%. Further increasing Zr content lowered the interlayer exothermicity and weakened the interfacial reaction. The cracks emerged again and became continuous when further increasing the Zr content. When the Zr content was 20 wt.%, the joint shear strength dropped to only 3.2 MPa.

4 Conclusions

- (1) A Ni–Al–Zr interlayer was designed according to theoretical calculation and experiment. Calculation showed that the $T_{\rm ad}$ of Ni–Al interlayer was 1912 K. The addition of Zr slightly lowered the ignition temperature and decreased the interlayer exothermicity.
- (2) The addition of Zr played a crucial role in the successful joining of $C_{f'}Al$ composites and TC4 alloy. The interlayer products transformed from NiAl to NiAl + Ni₂AlZr + Ni₃Al₅Zr₂, which increased the joint density and enhanced the interfacial reactions. The typical joint microstructure is TC4/Ti₃Al + Ni-Al-Ti + Ni-rich NiAl/Ni₂AlZr + Ni₃Al₅Zr₂ + NiAl/Ni-rich NiAl/Ni₂Al₃/NiAl₃ + (Ni,Zr)Al₃/C_{f'}Al.
- (3) Zr content determined the interlayer exothermicity, interlayer products and the interfacial reactions, and thus had a significant effect on the joint microstructure and shear strength. Appropriate Zr content improved the joining quality and increased the joint strength. When the Zr content was 5 wt.% and the joining pressure was 2 MPa, the joint had a maximum shear strength of 19.8 MPa.

Acknowledgments

The authors gratefully acknowledge the financial supports from the National Natural Science Foundation of China (Nos. 51975149, 51905055), the Natural Science Foundation of Chongqing, China (No. cstc2020jcyj-msxmX0115), and the Fundamental Research Funds for the Central Universities Project, China (No. 2020CDJ-LHZZ-086).

References

- [1] SILVESTRONI L, SCITI D, ESPOSITO L, GLAESER A M. Joining of ultra-refractory carbides [J]. Journal of the European Ceramic Society, 2012; 32: 4469–4479.
- [2] SHEN Lei, LI Zhuo-ran, FENG Guang-jie, ZHANG Shu-ye,

- HE Peng. Self-propagating synthesis joining of C_{f}/Al composites and TC4 alloy using AgCu filler with Ni–Al–Zr interlayer [J]. Rare Metals, 2021, 40(7): 1817–1824.
- [3] LI Da-guang, CHEN Guo-qin, JIANG Long-tao, XIU Zi-yang, ZHANG Yun-he, WU Gao-hui. Effect of thermal cycling on the mechanical properties of C_f/Al composites [J]. Materials Science and Engineering A, 2013, 586: 330–337.
- [4] LEE M, CHOI Y, SUGIO K, MATSUGI K, SASAKI G. Effect of aluminum carbide on thermal conductivity of the unidirectional C_f/Al composites fabricated by low pressure infiltration process [J]. Composites Science and Technology, 2014, 97: 1–5.
- [5] FENG Guang-jie, LI Zhuo-ran, ZHOU Zhi, WANG Yu. Joining of C_f/Al composites and TiAl intermetallics by laser-induced self-propagating high-temperature synthesis using the Ni–Al–Zr interlayer [J]. Materials and Design, 2016, 110: 130–137.
- [6] FENG Guang-jie, LI Zhuo-ran, FENG Shi-cheng, SHEN Zhong-ke. Effect of Ti-Al content on microstructure and mechanical properties of C_f/Al and TiAl joint by laser ignited self-propagating high-temperature synthesis [J]. Transactions of Nonferrous Metals Society of China, 2015, 25: 1468-1477.
- [7] FENG G, LI Z, JACOB R J, YANG Y, WANG Y, ZHOU Z, SEKULIC D P, ZACHARIAH M R. Laser-induced exothermic bonding of carbon fiber/Al composites and TiAl alloys [J]. Materials and Design, 2017, 126: 197–206.
- [8] XU Wei-feng, MA Jun, LUO Yu-xuan, FANG Yue-xiao. Microstructure and high-temperature mechanical properties of laser beam welded TC4/TA15 dissimilar titanium alloy joints [J]. Transactions of Nonferrous Metals Society of China, 2020, 30: 160-170.
- [9] YANG Xin, WANG Wan-lin, MA Wen-jun, WANG Yan, YANG Jun-gang, LIU Shi-feng, TANG Hui-ping. Corrosion and wear properties of micro-arc oxidation treated Ti₆Al₄V alloy prepared by selective electron beam melting [J]. Transactions of Nonferrous Metals Society of China, 2020, 30: 2132–2142.
- [10] BIAN Hong, SONG Xiao-guo, HU Sheng-peng, LEI Yu-zhen, JIAO Yi-de, DUAN Shu-tong, FENG Ji-cai, LONG Wei-min. Microstructure evolution and mechanical properties of titanium/alumina brazed joints for medical implants [J]. Metals, 2019, 9(6): 644.
- [11] ALFONSO I, NAVARRO O, VARGAS J, BELTRÁN A, AGUILAR C, GONZÁLEZ G, FIGUEROA I A. FEA evaluation of the Al₄C₃ formation effect on the Young's modulus of carbon nanotube reinforced aluminum matrix composites [J]. Composite Structures, 2015, 127: 420–425.
- [12] DEAQUINO-LARA R, SOLTANI N, BAHRAMI A, GUTIÉRREZ-CASTAÑEDA E, GARCÍA-SÁNCHEZ E, HERNANDEZ-RODRÍGUEZ M A L. Tribological characterization of Al7075-graphite composites fabricated by mechanical alloying and hot extrusion [J]. Materials and Design, 2015, 67: 224-231.
- [13] QI L H, MA Y Q, ZHOU J M, HOU X H, LI H J. Effect of fiber orientation on mechanical properties of 2D-C_f/Al composites by liquid-solid extrusion following vacuum infiltration technique [J]. Materials Science and Engineering

- A, 2015, 625: 343–349.
- [14] RAWAL S P. Interface structure in graphite-fiber-reinforced metal-matrix composites [J]. Surface and Interface Analysis, 2001, 31: 692–700.
- [15] BIAN Hong, SONG Yan-yu, LIU Duo, LEI Yu-zhen, SONG Xiao-guo, CAO Jian. Joining of SiO₂ ceramic and TC4 alloy by nanoparticles modified brazing filler metal [J]. Chinese Journal of Aeronautics, 2019, 33: 3–10.
- [16] LI Zhuo-ran, FENG Guang-jie, XU Kai, ZHANG Xiang-long. Microstructure and formation mechanism of SHS joining between C_f/Al composites and TiAl intermetallic with Al–Ni–CuO interlayer [J]. Rare Metals, 2015, 34: 17–21.
- [17] FENG G, LI Z, ZHOU Z, YANG Y, SEKULIC D P, ZACHARIAH M R. Microstructure and mechanical properties of C_f/Al-TiAl laser-assisted brazed joint [J]. Journal of Materials Processing Technology, 2018, 255: 195-203.
- [18] WANG Yi-feng, FENG Guang-jie, WEI Yan, HU Bing-xu, DENG De-an. Bonding SiC_p/Al composites via laser-induced exothermic reactions [J]. Crystals, 2021, 11: 535.
- [19] FIEDLER T, BELOVA I V, BROXTERMANN S, MURCH G E. A thermal analysis on self-propagating high temperature synthesis in joining technology [J]. Computational Materials Science, 2012, 53: 251–257.
- [20] PASCAL C, MARIN-AYRAL R M, TÉDENAC J C. Joining of nickel monoaluminide to a superalloy substrate by high pressure self-propagating high-temperature synthesis [J]. Journal of Alloys and Compounds, 2002, 337: 221–225.
- [21] LONG Zhong-min, DAI Bo, TAN Shi-jie, WANG Yong, WEI Xian-hua. Transient liquid phase bonding of copper and ceramic Al₂O₃ by Al/Ni nano multilayers [J]. Ceramics International, 2017, 43: 17000–17004.
- [22] LIN Y C, NEPAPUSHEV A A, MCGINN P J, ROGACHEV A S, MUKASYAN A S. Combustion joining of carbon/ carbon composites by a reactive mixture of titanium and mechanically activated nickel/aluminum powders [J]. Ceramics International, 2013, 39: 7499-7505.
- [23] LI Zhuo-ran, FENG Guang-jie, WANG Shi-yu, FENG Shi-cheng. High-efficiency joining of C_f/Al composites and TiAl alloys under the heat effect of laser-ignited self-propagating high-temperature synthesis [J]. Journal of Materials Science and Technology, 2016, 32: 1111-1116.
- [24] SHI Jun-miao, WANG Qian, TIAN Xiao-yu, XIONG Jiang-tao, LI Jin-long, ZHANG Li-xia, FENG Ji-cai. Brazing of Gr/2024Al composite and TC4 using AgCuTi filler with the assist of Ti-Al-C-Cu interlayer [J]. Journal of Manufacturing Processes, 2019, 47: 211–218.
- [25] REN Xiao, CHEN Guo-qing, ZHOU Wen-long, WU Cheng-wei, ZHANG Jun-shan. Effect of high magnetic field on intermetallic phase growth in Ni–Al diffusion couples [J]. Journal of Alloys and Compounds, 2009, 472: 525–529.
- [26] ZHU P, LI J C M, LIU C T. Adiabatic temperature of combustion synthesis of Al–Ni systems [J]. Materials Science and Engineering A, 2003, 357: 248–257.
- [27] ZAREZADEH MEHRIZI M, BEYGI R, MOSTAAN H, RAOUFI M, BARATI A. Mechanical activation-assisted combustion synthesis of in situ aluminum matrix hybrid (TiC/Al₂O₃) nanocomposite [J]. Ceramics International, 2016,

42: 17089-17094.

- A, 2019, 759: 303-312.
- [28] WANG Yong-lei, WANG Wan-li, HUANG Ji-hua, YU Rui-hua, YANG Jian, CHEN Shu-hai. Reactive composite brazing of C/C composite and GH3044 with Ag-Ti mixed powder filler material [J]. Materials Science and Engineering
- [29] SONG Xin-rui, LI He-jun, ZENG Xie-rong. Brazing of C/C composites to Ti₆Al₄V using multiwall carbon nanotubes reinforced TiCuZrNi brazing alloy [J]. Journal of Alloys and Compounds, 2016, 664: 175–180.

C_f/Al 复合材料与 TC4 钛合金的激光诱导燃烧合成连接

冯广杰 1,2 ,李卓然 1 ,何 鹏 1 ,沈 磊 1 ,周 志 1

- 1. 哈尔滨工业大学 先进焊接与连接国家重点实验室,哈尔滨 150001;
 - 2. 重庆大学 材料科学与工程学院, 重庆 400044

摘 要:采用激光诱导燃烧合成连接方法实现 C_f/Al 复合材料和 TC4 钛合金的可靠连接。放热中间层的燃烧合成反应为连接过程提供所需能量。结合理论计算和实验,对 Ni-Al-Zr 中间层的化学成分进行优化设计,并对连接接头的显微组织和力学性能进行研究。结果表明,Zr 的加入轻微降低中间层的放热性,但显著提高连接质量,是实现可靠连接的关键。Ni-Al-Zr 中间层与母材反应,在 TC4 钛合金侧生成 $TiAl_3$ 反应层,在 $TiAl_3$ 反应层,在 $TiAl_3$ 反应层。 $TiAl_3$ 反应反应层。 $TiAl_3$ 反应反应层。 $TiAl_3$ 反应层。 $TiAl_3$ 反应定点。 $TiAl_3$ 反应反应系。 $TiAl_3$ 反应反应系。 $TiAl_3$ 反应定态。 $TiAl_3$ 反应反应系。 $TiAl_3$ 反应反应系。 $TiAl_3$ 反应反应系。 $TiAl_3$ 反应反应系。 $TiAl_3$ 反应反应系。 $TiAl_3$ 反应应系。 $TiAl_3$ 反应反应系。 $TiAl_3$ 反应反应系。 $TiAl_3$ 反应反应系。 $TiAl_3$ 反应反应系。 $TiAl_3$ 反应应系。 $TiAl_3$ 反应应系。

关键词: C_f/Al 复合材料; TC4 钛合金; 燃烧合成连接; 界面显微组织; 剪切强度

(Edited by Wei-ping CHEN)